

Stator Optimization of 6-phase Claw-Pole Alternators Using Asymmetric Winding Arrangements

S. Schulte, C. Kaehler, C. Schlensok, G. Henneberger

Institute of Electrical Machines, RWTH Aachen University
 Schinkelstraße 4, 52062 Aachen, Germany, phone: (+49)-(0)241-8097636, fax: (+49)-(0)241-8092270,
 e-mail: stephan.schulte@iem.rwth-aachen.de

This article is dedicated to Prof. Gerhard Henneberger, who is released into his well deserved retirement with gratitude and appreciation for his meritorious scientific work.

I. ABSTRACT

Automotive applications are generally designed to reliable function and to low costs. Efforts to reduce noise, increase efficiency and expand duty cycles of electrical machines become of increasing importance and therefore call for optimized machine designs. Sophisticated machine concepts require long finite element analysis (FEA) computing times for the electromagnetic design and optimization processes.

A combination of different simulation approaches turns out to be a mighty means to decrease the total computing time and therefore costs significantly. Time effective analytical methods, used for the pre-determination of reasonable machine configurations as well as circuit-based simulations (SPICE-oriented) are utilized additionally to finite element (FE) simulations.

The optimization process is not necessarily bound to approved machine designs, but allows for investigations in various machine-structure modifications. This paper deals with electric and electromagnetic design and optimization methods of a 6-phase claw-pole alternator with an asymmetric stator winding arrangement.

II. INTRODUCTION

The design of common 3-phase claw-pole alternators basically consists of the DC excited rotor with characteristic claw fingers and the stator, equipped with a 2-layer 3-phase winding. The alignment and the phasor diagram of the stator windings are shown in Fig. 1 a,b. The expansion of the winding system to 6-phases reduces DC-link current ripples of the rectifier and therefore expands the duty cycle of the rectifier components. Besides current ripple reduction, the utilization of 6-phases reduces demands on ampacity of components of each phase. However, acoustic advantages will come along as a benefit.

III. BASIC STRUCTURE

The considered 6-phase winding consists of two separated parallel 3-phase windings (Fig. 2 a,b). The stator of the 6-phase machine consists of 72 slots, resulting in a slot pitch of the stator teeth of $\gamma = 5^\circ$. Due to cost minimization the

number of stator slots is fixed and not part of investigations. Moreover the winding distribution based on the slot number is subject of this paper

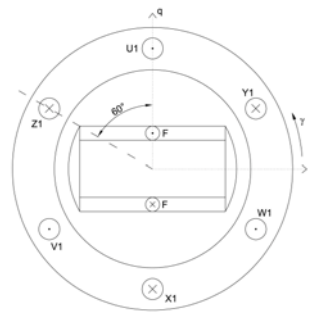


Fig. 1a: 3-phase salient-sole synchronous Machine.

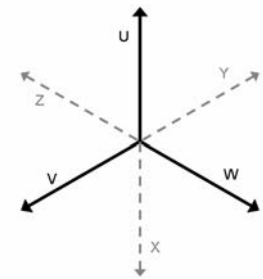


Fig. 1b: Accordant phasor orientation (3-ph).

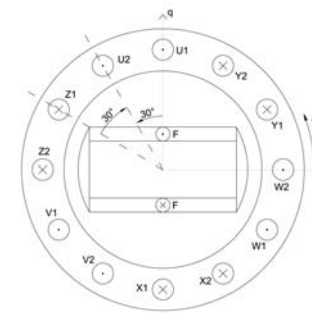


Fig. 2a: Expansion up to 6 stator phases.

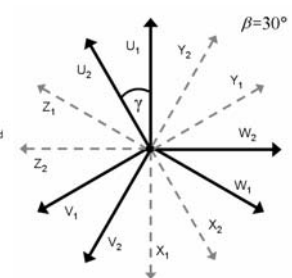


Fig. 2b: Accordant phasor orientation (6-ph).

Both separate 3-phase windings are shifted n -times the slot pitch $\beta = n \cdot \gamma$ (example in Fig. 3a,b and 4 a,b) to each other. The obvious arrangement of stator phases (Fig. 2 a,b) does not necessarily result in the best possible solution due to electric and magnetic requirements as well as to acoustic demands.

Asymmetric winding arrangements lead to both an asymmetric flux distribution and local saturation discrepancies in the stator. The determination of appropriate winding configurations (example: Fig. 3a,b and 4 a,b) is subject to computational analysis.

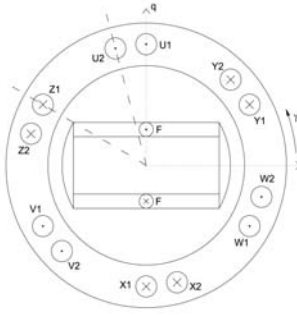


Fig. 3a: Varied stator arrangement.

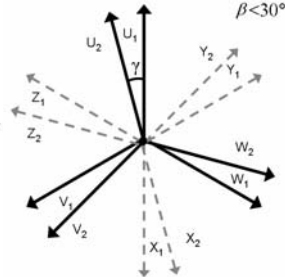


Fig. 3b: Accordant phasor orientation.

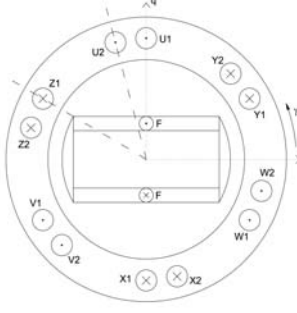


Fig. 4a: Varied stator arrangement.

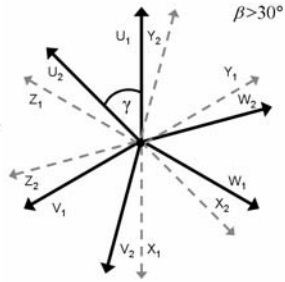


Fig. 4b: Accordant phasor orientation.

IV. APPROACH

i. ELECTRIC OPTIMIZATION

a) Preliminary Studies

In a first step of the optimization process, a set of different winding arrangements is selected with respect to given electric requirements.

Analytical means [1] as well as simulation tools [2] are utilized for this purpose.

At this early stage of design, phase currents of the alternator are assumed to be sinusoidal shaped for simplification reasons. This approximation is considered reasonable for the entire speed and excitation ranges. Phase current equations for both winding systems (index 1 and 2 in figures 2-4) are based on (1), (2). The implementation in Matlab [1] is brief (illustration in Fig. 5, top).

$$i_{1\ k+1} = \hat{I} \cdot \sin\left(\omega t + \frac{2 \cdot k \cdot \pi}{3}\right) \quad (1)$$

$$i_{2\ k+1} = \hat{I} \cdot \sin\left(\omega t + \beta + \frac{2 \cdot k \cdot \pi}{3}\right) \quad (2)$$

with the displacement angle β , $k = 0, 1, 2$

The influence of inductive coupling of other phases and the synchronous generated voltage is not considered at this stage. This approximation is reasonable for both considered speed and excitation ranges entirely.

The accordant DC-link current (Fig. 5, bottom) ensues to:

$$i_{DC-Link} = \sum_1^2 i_{UVW}(t). \quad (3)$$

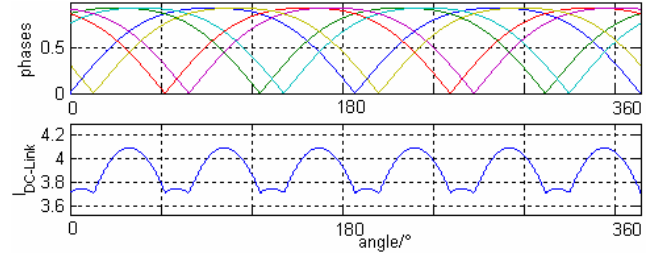


Fig. 5: $I_{1,2k}$ (top), $I_{DC-link}$ (bottom), 45° displaced.

At $\beta = 0$ the machine behaves as a double 2-layer 3-phase machine concerning current magnitude and frequency. If the angular displacement amounts $\beta = 30^\circ$, the DC-link current is of double frequency compared to the 3-phase case. All other winding displacement-compositions $0^\circ < \beta < 30^\circ$ require Fourier analysis for the determination of the fundamental frequency and higher harmonics.

Due to counteracting inductive influences of the phase currents, peak values of both phase current and DC-link current vary with β .

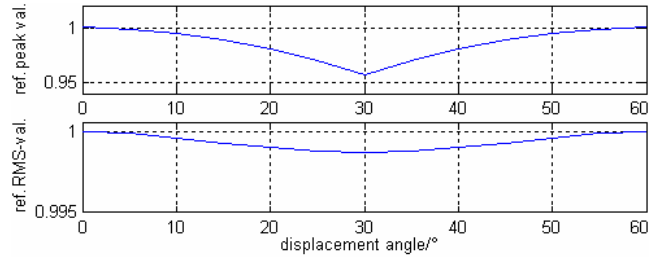


Fig. 6: Referred peak (top), RMS (bottom) values of $I_{1,2k}$, symmetry range of $0^\circ \leq \beta \leq 60^\circ$ displacement

It turns out, that a significant drop of current peak values ($\approx 5\%$) has minor influence on the accordant rms value, as Fig. 6 shows.

Since a reduction of peak values is desirable from the electrical point of view, winding displacements are most reasonable in the range of $\beta_{min} \leq 30^\circ \leq \beta_{max}$, stating the applicable symmetry range at the same time.

b) Detailed Curve Sketching

Other than for the simplified preliminary studies, mainly covering the macro-structural correlation of the winding system with the environmental vehicle power supply system, the curve sketching covers the internal machine behavior. For the detailed characteristic analysis, waveform simplifications are no longer feasible. Mutual inductive influences of the stator-phase currents, varying with the displacement angle β , effect the shape of the phase currents, i.e. the magnitude and the frequency. Therefore the harmonic analysis requires an authentic description of the current waveforms, taking particular winding arrangements into account.

The entire set of differential equations, describing the full machine behavior, contains currents (4)-(5), flux linkage (6), position dependent inductances (7) and motion equations (8)-(9) must be set up to describe the machine behavior entirely.

Different from the simplified pre-investigations, being subject to Matlab simulations, the entire differential equation set, stating a behavioral machine model is realized in VHDL-AMS [3]. VHDL-AMS is a standardized hardware description language for modeling of analog and mixed signal devices.

VHDL-AMS was originally developed for the modeling of integrated circuits. It turned out to be a mighty and powerful means for the modeling of almost any kind of electric and electromagnetic component (mechanical, fluid and thermal models are also possible), so that the AMS extension [5] has been added to the IEEE standard.

$$\left. \begin{aligned} i_{U1} &= \frac{\psi_{U1}}{L_{U1}} - i_{V1} \cdot \frac{L_{U1V1}}{L_{U1}} - i_{W1} \cdot \frac{L_{U1W1}}{L_{U1}} - i_{U2} \cdot \frac{L_{U1U2}}{L_{U1}} - i_{V2} \cdot \frac{L_{U1V2}}{L_{U1}} - i_{W2} \cdot \frac{L_{U1W2}}{L_{U1}} - i_F \cdot \frac{L_{U1F}}{L_{U1}} \\ i_{U2} &= \frac{\psi_{U2}}{L_{U2}} - i_{U1} \cdot \frac{L_{U1U2}}{L_{U2}} - i_{V1} \cdot \frac{L_{V1U2}}{L_{U2}} - i_{W1} \cdot \frac{L_{W1U2}}{L_{U2}} - i_{V2} \cdot \frac{L_{U2V2}}{L_{U2}} - i_{W2} \cdot \frac{L_{U2W2}}{L_{U2}} - i_F \cdot \frac{L_{U2F}}{L_{U2}} \end{aligned} \right\} \quad (4)$$

$$i_F = \frac{\psi_F}{L_F} - i_{U1} \cdot \frac{L_{U1F}}{L_F} - i_{V1} \cdot \frac{L_{V1F}}{L_F} - i_{W1} \cdot \frac{L_{W1F}}{L_F} - i_{U2} \cdot \frac{L_{U2F}}{L_F} - i_{V2} \cdot \frac{L_{V2F}}{L_F} - i_{W2} \cdot \frac{L_{W2F}}{L_F} \quad (5)$$

$$\left. \begin{aligned} \psi_{U1} &= \int (u_{U1} - i_{U1} \cdot R_{U1}) dt \Leftrightarrow u_{U1} = i_{U1} \cdot R_{U1} + \frac{d\psi_{U1}}{dt} \\ \psi_{U2} &= \int (u_{U2} - i_{U2} \cdot R_{U2}) dt \Leftrightarrow u_{U2} = i_{U2} \cdot R_{U2} + \frac{d\psi_{U2}}{dt} \end{aligned} \right\} \quad (6)$$

analogous for phase V1, V2, W1, W2 and excitation F

$$\left. \begin{aligned} L_{U1F} &= L_{FS} \cdot \cos\left(\gamma + \frac{\pi}{12} - \frac{2 \cdot k \cdot \pi}{3}\right), k=0 \\ L_{U2F} &= L_{FS} \cdot \cos\left(\gamma - \frac{\pi}{12} - \frac{2 \cdot k \cdot \pi}{3}\right), k=0 \end{aligned} \right\} \quad (7)$$

analogous for phase V1, V2 ($k=1$) and W1, W2 ($k=2$)

$$\gamma = \gamma_0 + \int \omega dt \Rightarrow \gamma - \gamma_0 + \int \omega dt = 0 \quad (8)$$

$$\alpha = \frac{1}{J} \cdot (M_i - M_w) \quad (9)$$

The VHDL-AMS 6-phase claw-pole alternator machine model is simulated in a simplified vehicle power supply network, shown in Fig. 7.

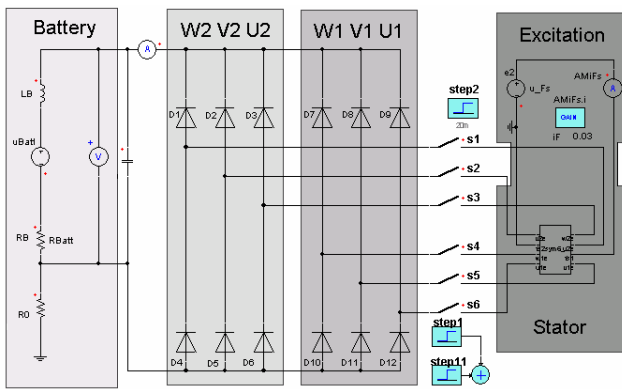


Fig. 7: Simplorer simulation sheet, VHDL machine model.

This simulation environment contains the external excitation circuit, an uncontrolled B12 rectifier bridge, the battery and the simulated load behavior of other components, and is entirely implemented and embedded in Simplorer [2].

The vehicle-power supply-simulation of the VHDL-AMS implemented alternator is used to check on sufficient

performance of power demands such as current limitation or torque exertion for verification purposes.

The combination of the analytical equation set up in the VHDL-AMS machine model and the simulation in Simplorer allows for comfortable and unrestricted parameter access. Any variable or parameter is accessible, can be plotted (Fig. 8), modified, or adapted for optimization purposes in further simulations.

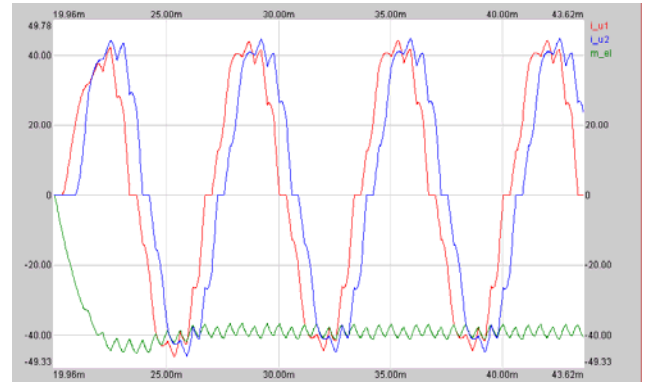


Fig. 8: Simplorer plot of currents i_{U1} , i_{U2} and torque M_{el} .

For the considered machine design: mutual angular displacement of both stator-winding systems are modified by simple parameter variation. The stator winding arrangement is varied by adapting the mutual inductances between stator phases of both systems #1 and #2, as well as the mutual inductances between stator and rotor. Particular steps of integer pole pitch widths are based on this displacement (steps of 5° for the considered alternator constructed with 72 stator slots).

The variation of the number of windings or the winding profile as such is also conceivable, affecting internal parameters, such as the flux or the magnetomotive force. Besides verification purposes, analysis opportunities are provided. Each variable of the analytically implemented

VHDL-AMS model can be saved for post-processing means.

The VHDL-AMS machine-model implementation provides saving of results of arbitrary variables in ASCII files – here the stator currents and torque characteristics. The ASCII files (Fig. 9) contain equidistant time base and accordant current and torque values column wise, tab separated each.

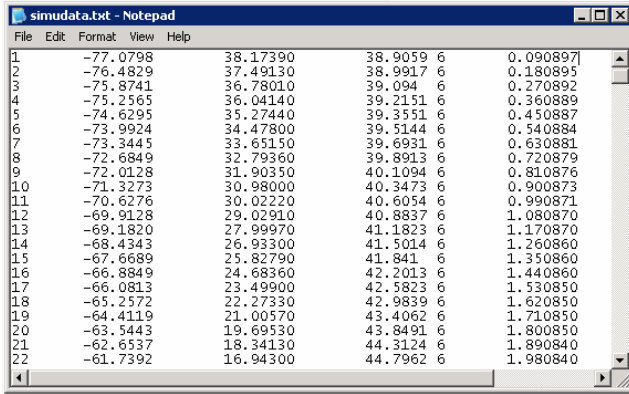


Fig. 9: Simulation data in ASCII file.

The choice of using a plain text format for the simulation result target files offers universal utilization opportunities for further processing, largely independent from manufacturer specific data formats.

The described simulation results in ASCII representation state the input files for the harmonic analysis of the considered detailed investigation. Therefore, the simulation results are imported into the Matlab workspace with no more file format adaptation needed. Workspace content adaptation merely affects required cut outs of transient phenomena.

Torque and current characteristics – the latter to be squared for stator force estimation – are processed using a Matlab implemented Fourier analysis routine.

This routine auto detects an entire cycle of the characteristic to be analyzed; solely the accordant resolution needs to be defined manually.

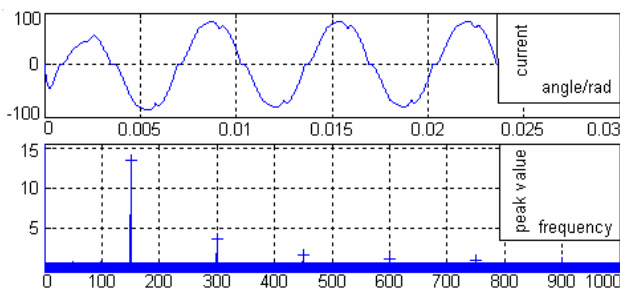


Fig. 10: Current i_{U1} waveform (top), FFT (bottom).

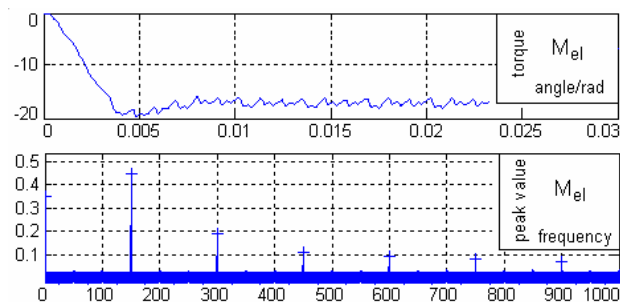


Fig. 11: Torque M characteristic (top), FFT (bottom).

Appliance of the analytically implemented Fourier analysis leads to frequency results showing contained fundamental wave and harmonics as exemplarily illustrated for stator current i_{U1} and torque M_{el} in Fig. 10 and 11.

ii. MAGNETIC OPTIMIZATION

The resulting configuration of the electrical pre-designing process does not necessarily need to state a reasonable choice from the magnetic point of view, so that reasonable winding arrangements resulting from the analytical optimization process need to be evaluated due to their magnetic behavior using numerical methods.

Although current peak-values are significantly decreased by duplicating the number of phases, the angular displacement of both winding systems may lead to local flux superelevation, based on disadvantageous winding correlation.

Besides superelevation, asymmetric saturation in stator teeth and yoke may occur for the considered machine design, based on parasitic flux distribution, ensuing in unwanted and parasitic effects such as torque ripples, noise or local eddy current accumulation.

The resulting configuration of the electrical optimization process does not necessarily need to state a reasonable choice from the magnetic point of view

The given machine type, featuring variable stator winding arrangements, results in an accordant asymmetric flux distribution. This may lead to desirable benefits, such as a reduction of noise and on the other hand to unwanted and parasitic effects.

Therefore, numerical methods, such as FE simulations, are applied to double check both on proper magnetic design (see Fig. 12) as well as on correct results of the analytical calculations of electrical and mechanical values.

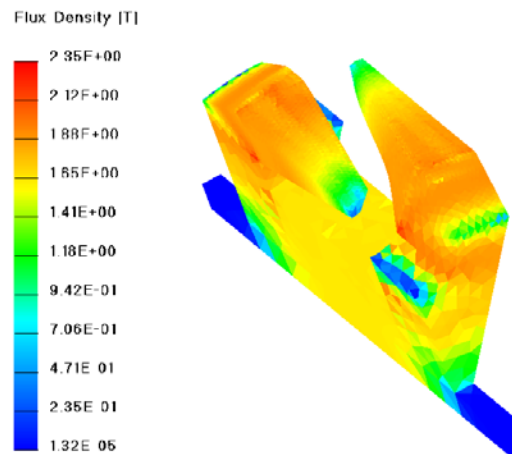


Fig. 12: Flux density in rotor out of FE simulation.

The given example of a 6-phase claw-pole alternator is magnetically designed using ANSYS [4] for modeling and meshing and a self-developed object-oriented solver environment *i*MOOSE [5] with static and transient 3D solvers for computation, post-processing and visualization. The *i*MOOSE package is partly open source and is subject to further development.

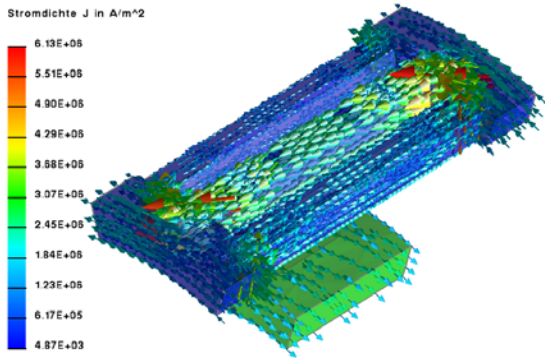


Fig. 13: Current density in stator and field windings.

V. CONCLUSION

The variation of the stator winding arrangement of a 6-phase claw-pole alternator enables opportunities for electric, magnetic, and acoustic optimization. A method to design and optimize the stator arrangement of a 6-phase claw-pole alternator is presented.

At first this scheme consists of analytical pre-design for a pre-selection of reasonable stator-winding configurations. SPICE-oriented simulation concepts determine the real machine behavior running in a vehicle power supply network model, with regular duty cycles as well as fault scenarios being applicable.

Electromagnetic design as well as a verification of the pre-design iteration-step is performed using FE simulation. The performed FE analysis of the machine model enables powerful post-processing opportunities, such as investigations on force, acoustics and structure-dynamics.

VI. REFERENCES

- [1] Matlab/Simulink, homepage: www.mathworks.com
- [2] Simplorer, Ansoft Inc., homepage: www.ansoft.com
- [3] VHDL-AMS: Very high speed Hardware Description Language – Analog and Mixed Signals, IEEE 1076.1-1993
- [4] ANSYS Inc., homepage: www.ansys.com
- [5] iMOOSE – innovative Modern Object-Oriented Solver Environment, homepage: www.imoose.de
- [6] C. Kaehler, G. Henneberger, Calculation of the mechanical and acoustic behaviour of a claw-pole alternator in double and single star connection, 4th International Symposium on Advanced Electromechanical Motion Systems, Electromotion 2001
- [7] C. Kaehler, G. Henneberger, Calculation of the differences in the acoustical behaviour of a claw-pole alternator when connected in delta and star, 2nd International Seminar on Vibrations and Acoustic Noise in Electric Machinery, VANEM 2000